THE ASTROPHYSICAL JOURNAL, 503:L143–L146, 1998 August 20
© 1998. The American Astronomical Society. All rights reserved. Printed in U.S.A.

ASCA OBSERVATION OF THE SUPERSOFT X-RAY SOURCE CAL 87

K. ASAI, T. DOTANI, AND F. NAGASE
Institute of Space and Astronautical Science, 3-1-1, Yoshinodai, Sagamihara, Kanagawa 229-8510, Japan;
asai@astro.isas.ac.jp, dotani@astro.isas.ac.jp, nagase@astro.isas.ac.jp
K. EBISAWA, K. MUKAI, AND A. P. SMALE
Laboratory for High Energy Astrophysics, NASA/Goddard Space Flight Center, Greenbelt, MD 20771
AND
T. KOTANI
Institute of Physical and Chemical Research (RIKEN), Saitama 351-0198, Japan
Received 1998 April 21; accepted 1998 June 23; published 1998 July 22

ABSTRACT

We have investigated the energy spectrum and the orbital modulation of the supersoft X-ray source CAL 87 using the *ASCA* satellite. We have detected a deep absorption edge at $0.85^{+0.02}_{-0.01}$ keV superposed on a continuum that can be approximated with an absorbed blackbody ($kT = 0.05^{+0.06}_{-0.01}$ keV). The edge structure may be produced by the highly ionized species of O VIII and O VII. Such deep edge structures from highly ionized heavy elements are expected for X-ray emission from a white dwarf with an envelope of stable hydrogen burning and strongly supports the model that a white dwarf with a large mass accretion rate is involved in the supersoft X-ray sources. Epoch-folding analysis reveals the presence of a partial X-ray eclipse with broad wings at orbital phase 0; the eclipse covers a quarter of the orbital phase and the X-ray flux decreases down to ~40% of the out-of-eclipse level. We discuss the possible cause of the partial eclipse, including the extended emission region due to the accretion disk corona, and the X-ray scattering site formed by the gas escaping from the binary system, where the gas is highly ionized by the large X-ray luminosity from the white dwarf.

Subject headings: binaries: close — binaries: eclipsing — stars: individual (CAL 87) — white dwarfs — X-rays: stars

1. INTRODUCTION

It has been established through *Einstein* and *ROSAT* observations that the supersoft X-ray sources (SSSs) constitute a distinct class of X-ray sources (Hasinger 1994; Kahabka & van den Heuvel 1997). They are characterized by a bolometric luminosity close to the 1 $M_\odot$ Eddington limit and a blackbody temperature between about 10 and 100 eV. SSSs are preferentially detected in the Magellanic Clouds, but some are found in the Galaxy. The most likely model for the SSS involves a white dwarf in a close binary system (van den Heuvel et al. 1992). When the mass accretion rate is high within a suitable range, stable hydrogen burning is expected in the envelope of the white dwarf. Such a white dwarf is suspected to show up as an SSS with characteristics described above. Although the results with *Einstein*, *ROSAT*, and *BeppoSAX* support this interpretation, direct evidence has not yet been obtained for the radiation from the nuclear-burning atmosphere of the white dwarf.

CAL 87 is one of the best studied SSSs located in the Large Magellanic Cloud (LMC). It is a binary system with an orbital period of 10.6 hr (Cowley et al. 1990). Cowley et al. (1990) reported the radial velocity variations of the He II lines and discussed the possibility that the system contains a black hole. *ROSAT* observations show that the source has a very soft spectrum with a blackbody temperature of ~30–50 eV (Kahabka, Pietsch, & Hasinger 1994). It is very luminous ($\geq 5 \times 10^{38}$ ergs s^{-1}) and suffers from a large photoelectric absorption ($N_H \sim 10^{22}$ cm^{-2}). The results from *BeppoSAX* give a more reasonable constraint to the source luminosity ($\geq 4 \times 10^{36}$ ergs s^{-1}) by blackbody model fitting including an O VIII edge at 0.87 keV (Parmer et al. 1997). The optical light curve shows two minima, one deep and one shallow, per orbit (Cowley et al. 1990). A shallow eclipse is also detected in X-rays, which coincides with the primary minimum in the optical band (Schmitdke et al. 1993).

In this Letter, we report detection of the clear absorption edge in the energy spectrum and of the partial eclipse with broad wings. The former may be direct evidence of radiation from a hot white dwarf. Detailed spectral analysis based on the white dwarf model atmosphere will be presented elsewhere (Ebisawa et al. 1998).

2. OBSERVATIONS AND DATA REDUCTION

We observed CAL 87 with *ASCA* from 1996 September 6, 6:00 (UT) through September 8, 8:30, for a net exposure of 80 ks. *ASCA* (Tanaka, Inoue, & Holt 1994) carries two kinds of detectors: the solid-state imaging spectrometer (SIS) (Burke et al. 1994; Yamashita et al. 1997) and the gas imaging spectrometer (GIS) (Ohashi et al. 1996; Makishima et al. 1996). The SIS has higher sensitivity in the low-energy band and has a higher energy resolution than the GIS. CAL 87 was clearly detected with the SIS, while the detection was marginal with the GIS. Therefore, we use only the SIS data for the present analysis. SIS data were taken in the 1 CCD faint mode with a time resolution of 4 s. We rejected any data taken at low elevation angles from the bright Earth (less than 15°), during the Earth occultation of the source and the South Atlantic Anomaly. The spectra and light curve were calculated using the X-ray event data extracted from the 3′ radius circular region centered on the source. Because CAL 87 is relatively dim in the *ASCA* band (0.45–10 keV), careful background subtraction was needed. We compared the local background level of the field including CAL 87 with the high-latitude blank-sky region. The former is found to have higher background than the blank-sky region by 6%–9% for the energy band of 0.5–1.2 keV. There-

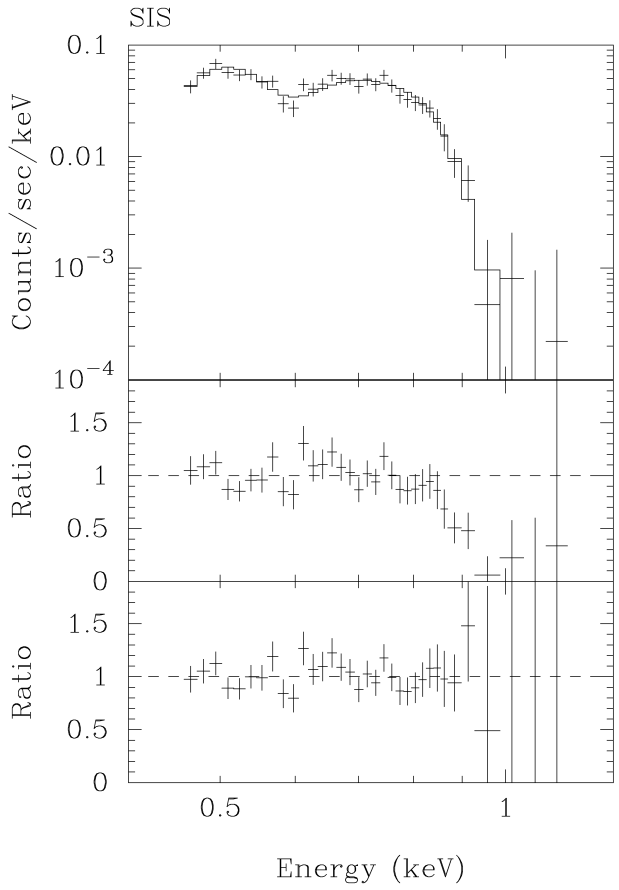


FIG. 1.—*Top:* Energy spectrum of CAL 87 obtained with the *ASCA* SIS. Data (*crosses*) from the two sensors, SIS-0 and SIS-1, are added. The best-fit model function, a blackbody with an absorption edge, is also plotted as a histogram. *Middle:* Ratio of the data to the model spectrum of a simple absorbed blackbody. The model is optimized with the data below 0.8 keV and is extrapolated toward higher energies. The edge structure is clearly seen at ~0.85 keV. *Bottom:* Ratio of the data to the model spectrum. The model is a blackbody with an absorption edge at 0.85 keV, as in the top panel.

fore, we used the data extracted from the annulus region (radius 5′–3′) centered on CAL 87 as the background.

3. ANALYSIS AND RESULTS

3.1. *Spectral Analysis*

We have calculated an average energy spectrum of CAL 87 using all of the data obtained from the *ASCA* observations. The energy spectrum (Fig. 1) is dominated by sub-keV photons, and no significant source photons were detected above 1 keV. We performed model fitting to get a rough description of the energy spectrum. We first tried a blackbody model with a cold gas absorption. The galactic foreground contribution to the cold gas absorption was fixed at 8×10^{20} cm^{-2} (Kahabka et al. 1994), and the excess absorption over the galactic value was estimated in the fitting. We assume that the cold matter responsible for the excess absorption has a metallicity of 0.5 $Z_{\odot}$ to approximate the abundance in LMC. We used a summed energy spectrum of SIS-0 and SIS-1 in the fitting to improve statistics. We found that a simple absorbed blackbody does not fit the observed spectra very well (reduced $\chi^2 = 1.44$ for 33 degrees of freedom [dof]). This model is rejected at a confidence limit of 95%. Inspection of the fit residual shows the presence of a sharp feature between 0.8 and 0.9 keV. To see the feature well, we restricted the fit below 0.8 keV and extrapolated the best-fit model above 0.8 keV. The result is shown in Figure 1 (*middle*); the presence of the absorption edge feature at ~0.85 keV is clear.

TABLE 1
FITTING RESULTS WITH *ASCA*

kT (keV)	Radius[a] (10^4 km)	$N_{\rm H}$ (10^{21} cm^{-2})	$E_{\rm edge}$ (keV)	τ	χ^2_ν (dof)
$0.05^{+0.06}_{-0.01}$	0.005–20	7^{+5}_{-6}	$0.85^{+0.02}_{-0.01}$	>2	0.86 (31)

[a] Source distance of 55 kpc is assumed.

Next, we tried to add an absorption edge to the blackbody model in order to improve the fit. The result is shown in Figure 1, and the best-fit parameters are summarized in Table 1. As seen from the figure, a deep absorption edge at 0.85 keV with the blackbody continuum can fit the energy spectrum well. The presence of the edge is very significant statistically. According to the *F*-test, the reduction of χ^2 is large enough [corresponding to $F(2, 31) = 24$] to justify the addition of the absorption edge at the confidence limit of greater than 99.9%. The large errors of parameters are due mainly to the coupling between the blackbody temperature and the absorption column density. We have tried to constrain the bolometric luminosity and the size of the emission region from the blackbody model fitting with the absorption edge. Allowed ranges of the parameters are very wide, and the bolometric luminosity and the size of the emission region are $\geq 3 \times 10^{36}$ ergs s^{-1} and $(0.005–20) \times 10^4$ km, respectively, for the assumed distance of 55 kpc.

3.2. *Orbital Modulation*

We have searched for the orbital variations of X-ray intensity in the SIS data using the epoch-folding technique. We find a clear peak in χ^2 space (maximum $\chi^2_\nu = 5.7$ with 15 dof) at the period of 10.4 ± 0.5 hr, which is consistent with the value obtained by Alcock et al. (1997). Figure 2 shows the folded light curves in two energy bands, 0.45–0.65 and 0.65–1.0 keV, using the ephemeris (T_0 = HJD 2450111.5144 + 0.44267714n) by Alcock et al. (1997). Note that there are no significant source photons above 1 keV (§ 3.1). As seen in the folded light curves, a clear decrease in X-ray flux is detected at around phase 0, which corresponds to the primary eclipse in the optical band. Thus the decrease is considered to be due to the partial eclipse of the X-ray source. The eclipse seems to have very broad wings similar to those seen in the optical data (Schmidtke et al. 1993), but the asymmetry found in the optical data is not very clear in X-ray data. A secondary eclipse at phase 0.5 observed in the optical has not been detected in the *ASCA* data.

The eclipse profile is not very clear in the higher energy band (0.65–1.0 keV). To confirm the energy dependence, we have fitted a triangular function to the eclipse light curve. The triangular function is found to represent the eclipse profile in the lower energy band satisfactorily ($\chi^2_\nu = 1.17$ with 17 dof). The best-fit model function is also plotted in Figure 2. The depth of the eclipse (i.e., the decrease of the flux from the out-of-eclipse level) is found to be 60^{+20}_{-10} %. If we fit the eclipse profile in the higher energy band with the same function fixing the eclipse depth to 60%, the fit is not acceptable ($\chi^2_\nu = 1.55$ with 21 dof). The fit is slightly improved if we optimize the eclipse depth to give a minimum χ^2 ($\chi^2_\nu = 1.20$ with 20 dof);

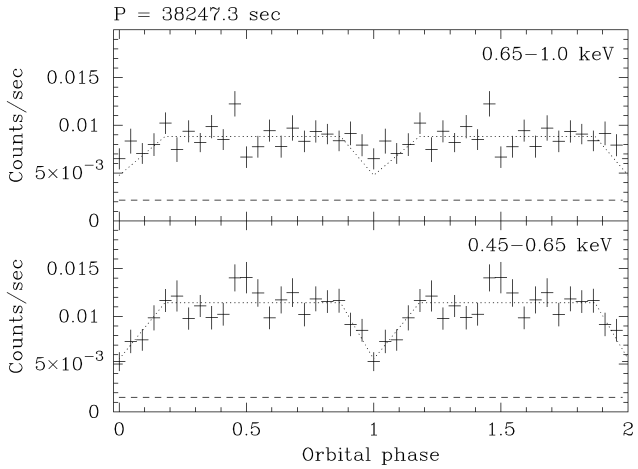


FIG. 2.—Folded light curves of CAL 87 with the ephemeris by Alcock et al. (1997). The top panel shows the light curve in 0.65–1.0 keV, and the bottom panel shows the light curve in 0.45–0.65 keV. Broken lines indicate the background level. Note the presence of the partial eclipse at phase 0. The dotted line in the lower panel is the best-fit triangular function to the eclipse profile. The function is also plotted in the top panel, but the depth of the eclipse is fixed to the value obtained from 0.45–0.65 keV data. The discrepancy between the data and the model in the top panel indicates that the depth of the eclipse may be reduced in the higher energy band.

an F-test [$F(1, 20) = 7.1$] shows that this decrease of χ^2 is significant at a 98% confidence limit. The best-fit eclipse depth is found to be 26% ± 20%. From the above analysis, we can say that there is a hint of energy dependence in the eclipse depth, although its statistical significance is not very high.

We have compared the energy spectrum during the eclipse (orbital phase 0.84–1.16) with that of the persistent emission (orbital phase 0.2–0.8). However, because of the limited statistics, the difference of the energy spectra is not clear. If we assume that the eclipse is produced by the photoelectric absorption, as indicated by its energy dependence, the excess absorption column density corresponds to $\sim 5 \times 10^{20}$ cm^{-2} ($Z = 0.5\ Z_{\odot}$).

4. DISCUSSION

We have detected a clear absorption edge at $0.85^{+0.02}_{-0.01}$ keV in the energy spectrum of CAL 87 for the first time. The presence of this edge structure in the spectrum is expected for emission from a hot white dwarf with a stable hydrogen-burning envelope (Heise, van Teeseling, & Kahabka 1994; van Teeseling, Heise, & Kahabka 1996). Model calculations show that the edge structures originate from hydrogen- or helium-like ions of carbon, nitrogen, or oxygen. The observed edge energy (0.85 keV) tends to be slightly lower than that of O VIII (0.871 keV), although the difference is marginal, and a small contribution from O VII (0.739 keV) is suspected. To investigate this point, we tried to include two oxygen K edges with the edge energies fixed to 0.739 and 0.871 keV, respectively, in the blackbody model. The fit ($\chi^2_{\nu} = 0.80$ for 31 dof) was as good as a single-edge model, and the best-fit absorption depths were $\tau = 0.5 \pm 0.4$ for O VII and $\tau > 3$ for O VIII, respectively. Because no significant source photons were detected above ~0.9 keV, we could obtain only the lower limit to the optical depth for O VIII. Thus, the observed edge may be in fact produced by the mixture of a shallow edge of O VII and a deep edge of O VIII.

Detection of the strong absorption edge structures due to highly ionized oxygen is considered to be direct evidence for a hot white dwarf as the origin of CAL 87 and most likely also in the other SSS. It was once suggested that a black hole or a neutron star may be involved in the SSS (Cowley et al. 1990; Kylafis & Xilouris 1993). However, the deep edge structure as detected from CAL 87 can be naturally explained only by the radiation from a white dwarf envelope rather than a black hole or a neutron star. In the hot white dwarf atmosphere, the temperature range in which O VIII coexists with a small fraction of O VII is considered to be 60–80 eV (e.g., Ebisawa et al. 1996). This is consistent with the range of blackbody temperatures that we derived from the model fitting, and thus supports the white dwarf atmospheric spectral model.

We have also detected a clear partial eclipse in the folded light curve of CAL 87 with *ASCA*. The eclipse has very broad wings, which confirms earlier indications by *ROSAT* (Schmitdke et al. 1993). The X-ray eclipse center just coincides with phase 0, so the eclipse is most probably due to the occultation of the white dwarf by the companion (i.e., mass-donating) star. However, one might suspect that it is difficult to produce such a partial eclipse by the occultation of the companion, since the white dwarf is 2 orders of magnitude smaller than the companion star, and that the eclipse would become a total eclipse. Such a contradiction may be resolved if either an extended X-ray emission region or an extended X-ray scattering region is involved in the eclipse. To identify the principal mechanism that produces the partial eclipse, we consider two extreme cases: (1) CAL 87 has an extended emission region, and the companion star just blocks X-rays and (2) CAL 87 is a point X-ray source, and the companion star has an extended atmosphere and/or winds to attenuate X-rays by absorption or scattering.

First, we consider case 1. To explain the duration of the eclipse (about a quarter of the orbital period), the X-ray emission region (radius R_X) and the companion (radius R_c) need to satisfy the following relation: $R_X + R_c = a \cos(\pi/4)$. Here, a is the binary separation ($=2.2 \times 10^{11}$ cm), and the inclination angle of 90° is assumed. Using the radius of the companion star, $R_c = 1 \times 10^{11}$ cm (e.g., Schandl, Meyer-Hofmeister, & Meyer 1997), we obtain $R_X = 6 \times 10^{10}$ cm as the radius of the X-ray emitting region. Such an extended emission region may be realized if the white dwarf were embedded in the so-called accretion disk corona (ADC) (Hellier & Mason 1989). Since we see no sign of a point source eclipse in the X-ray light curve, the optical depth has to be large ($\tau \gg 1$), or the white dwarf must be permanently hidden from our direct view by the thickened outer disk. In either case, the size of the ADC has to be comparable with that of the white dwarf's Roche lobe (7×10^{10} cm; $M_{\rm WD}/M_{\rm companion} = 0.5$ is assumed). Such a large ADC will block our direct view to the accretion disk; according to Schandl et al. (1997), contribution from the accretion disk and the spray region is important in reproducing the optical light curve. If $\tau \gg 1$, this may therefore cause difficulties in explaining the optical light curves. We conclude that our case 1, the extended X-ray emission region due to the ADC, would only work if the optical depth is modest and the direct component is hidden. The observed X-rays must then be a small fraction of the intrinsic X-ray luminosity; the results of our spectral fitting are consistent with such a view.

Next, we consider case 2, that the extended absorption/scattering region produces the partial eclipse with broad wings. The observed depth of the eclipse (60^{+20}_{-10} %) corresponds to the

excess X-ray absorption of $N_{\rm H} \sim 5 \times 10^{20}$ cm^{-2}. Using the same relation as in case 1, we can calculate that the matter responsible for the excess absorption must have an extent of 3×10^{11} cm to explain the duration of the eclipse. This means that its location is also at least 3×10^{11} cm away from the white dwarf. Then, the ξ parameter of the material ($\equiv L_{\rm X}/nr^2$), which determines its ionization state, is estimated as $\xi \sim 10^5$ ($L_{\rm X} = 10^{37}$ ergs s^{-1}, $nr = 5 \times 10^{20}$ cm^{-2}, and $r = 3 \times 10^{11}$ cm are used). Such a large ξ value means that the matter is completely ionized and cannot contribute to the X-ray absorption. Thus, the X-ray absorption cannot be the cause of the eclipse, and the X-ray scattering needs to be involved instead.

The scattering optical depth necessary to produce the observed depth of the eclipse is about unity. Again, the X-ray scattering site needs to be extended as large as 3×10^{11} cm, which leads to the average number density of the X-ray scattering plasma to be of order 10^{12} cm^{-3}. Such an extended X-ray scattering site may be supported by the wind escaping from the binary system. If we assume a wind velocity of 10^7 cm s^{-1}, the mass-loss rate due to the wind would be $\sim 10^{-7}$ $M_\odot$ yr^{-1}. This is comparable to the mass-loss rate necessary to support the stable hydrogen burning in the white dwarf envelope. The mass transfer from the companion to the white dwarf, which occurs through the Roche lobe overflow, is considered to be unstable (van den Heuvel et al. 1992), and the mass supply from the companion may not balance, or exceed, the mass accretion rate. Under these circumstances, a significant fraction of the mass may not be able to accrete onto the white dwarf and escape from the binary system as a wind. The wind will become highly ionized due to the large X-ray luminosity from the white dwarf and will work as an X-ray scattering site to produce the partial eclipse with broad wings. Presence of such outflowing gas may be supported by the recent detection of the Balmer absorption line with a velocity of $\sim$80 km s^{-1} (Hutchings et al. 1998).

Although we have considered two extreme cases, both mechanisms may work together to produce the observed eclipse profile. For example, the eclipse profile near phase 0 may be determined by the ADC and the wings by the wind. In either mechanism, it is difficult to explain the energy dependence of the eclipse, if it really exists, since the X-ray scattering itself is energy independent. Data with higher statistical quality would be needed to study the energy dependence of the eclipse in more detail.

REFERENCES

Alcock, C., et al. 1997, MNRAS, 287, 699
Burke, B. E., Mountain, R. W., Daniels, P. J., Cooper, M. J., & Dolat, V. S. 1994, IEEE Trans. Nucl. Sci., 41, 375
Cowley, A. P., Shmidtke, P. C., Crampton, D., & Hutching, J. B. 1990, ApJ, 350, 288
Ebisawa, K., Asai, K., Mukai, K., Smale, A., Dotani, T., Hartmann, H. W., & Heise, J. 1996, in Supersoft X-Ray Sources, ed. J. Greiner (Lecture Notes in Physics; Berlin: Springer), 91
Ebisawa, K., et al. 1998, in preperation
Hasinger, G. 1994, in AIP Conf. Proc. 308, The Evolution of X-Ray Binaries, ed. S. S. Holt & C. S. R. Day (New York: AIP), 611
Heise, J., van Teeseling, A., & Kahabka, P. 1994, A&A, 288, L45
Hellier, C., & Mason, K. O. 1989, MNRAS, 239, 715
Hutchings, J. B., Crampton, D., Cowley, A. P., & Schmidtke, P. C. 1998, ApJ, in press
Kahabka, P., Pietsch, W., & Hasinger, G. 1994, A&A, 288, 538
Kahabka, P., & van den Heuvel, E. P. J. 1997, ARA&A, 35, 69
Kylafis, N. D., & Xilouris, E. M. 1993, A&A, 278, L43
Makishima, K., et al. 1996, PASJ, 48, 171
Ohashi, T., et al. 1996, PASJ, 48, 157
Parmar, A. N., Kahabka, P., Hartmann, H. W., Heise, J., Martin, D. D. E., Bavdaz, M., & Mineo, T. 1997, A&A, 323, L33
Schandl, S., Meyer-Hofmeister, E., & Meyer, F. 1997, A&A, 318, 73
Schmidtke, P. C., McGrath, T. K., Cowley, A. P., & Frattare, L. M. 1993, PASP, 105, 863
Tanaka, Y., Inoue, H., & Holt, S. S. 1994, PASJ, 46, L37
van den Heuvel, E. P. J., Bhattacharya, D., Nomoto, K., & Rappaport, S. A. 1992, A&A, 262, 97
van Teeseling, A., Heise, J., & Kahabka, P. 1996, in IAU Symp. 165, Compact Stars in Binaries, ed. J. van Paradijs, E. P. J. van den Heuvel, & E. Kuulkers (Dordrecht: Kluwer), 445
Yamashita, A., et al. 1997, IEEE Trans. Nucl. Sci., 44, 847